

Minimap2: fast pairwise alignment for long DNA sequences

Heng Li

Broad Institute, 415 Main Street, Cambridge, MA 02142, USA

ABSTRACT

Summary: Minimap2 is a general-purpose mapper to align long noisy DNA sequences against a large reference database. It targets query sequences of 1kb–100Mb in length with per-base divergence typically below 25%. Minimap2 is ~ 30 times faster than many mainstream long-read aligners and achieves higher accuracy on simulated data. It also employs concave gap cost and rescues inversions for improved alignment around potential structural variations.

Availability and implementation: <https://github.com/lh3/minimap2>

Contact: hengli@broadinstitute.org

1 INTRODUCTION

Single Molecule Real-Time (SMRT) sequencing technology and Oxford Nanopore technologies (ONT) produce reads over 10kbp in length at an error rate $\sim 15\%$. Several aligners have been developed for such data (Chaisson and Tesler, 2012; Li, 2013; Liu et al., 2016; Sović et al., 2016; Liu et al., 2017; Lin and Hsu, 2017; Sedlazeck et al., 2017). They are usually five times as slow as mainstream short-read aligners (Langmead and Salzberg, 2012; Li, 2013). We speculated there could be substantial room for speedup on the thought that 10kb long sequences should be easier to map than 100bp reads because we can more effectively skip repetitive regions, which are often the bottleneck of short-read alignment. We confirmed our speculation by achieving approximate mapping 50 times faster than BWA-MEM (Li, 2016). Suzuki (2016) extended our work with a fast and novel algorithm on generating detailed alignment, which in turn inspired us to develop minimap2 towards higher accuracy and more practical functionality.

2 METHODS

Minimap2 is the successor of minimap (Li, 2016). It uses similar indexing and seeding algorithms, and furthers it with more accurate chaining and the ability to produce detailed alignment.

2.1 Chaining

An *anchor* is a 3-tuple (x, y, w) , indicating interval $[x - w + 1, x]$ on the reference matching interval $[y - w + 1, y]$ on the query. Given a list of anchors sorted by ending reference position x , let $f(i)$ be the maximal chaining score up to the i -th anchor in the list. $f(i)$ can be calculated with dynamic programming (DP):

$$f(i) = \max \left\{ \max_{i > j \geq 1} \{f(j) + d(j, i) - \gamma(j, i)\}, w_i \right\} \quad (1)$$

where $d(j, i) = \min \{ \min\{y_i - y_j, x_i - x_j\}, w_i \}$ is the number of matching bases between the two anchors. $\gamma(j, i) > 0$ is the gap cost. It equals ∞ if $y_j \geq y_i$ or $\max\{y_i - y_j, x_i - x_j\} > G$ (i.e. the distance between two anchors is too large); otherwise

$$\gamma(j, i) = \gamma'(\max\{y_i - y_j, x_i - x_j\} - \min\{y_i - y_j, x_i - x_j\})$$

In implementation, a gap of length l costs $\gamma'(l) = \alpha \cdot l + \beta \log_2(l)$. For m anchors, directly computing all $f(\cdot)$ with Eq. (1) takes $O(m^2)$ time.

Although theoretically faster chaining algorithms exist (Abouelhoda and Ohlebusch, 2005), they are inapplicable to generic gap cost, complex to implement and usually associated with a large constant. We introduced a simple heuristic to accelerate chaining.

We note that if anchor i is chained to j , chaining i to a predecessor of j is likely to yield a lower score. When evaluating Eq. (1), we start from anchor $i - 1$ and stop the evaluation if we cannot find a better score after up to h iterations. This approach reduces the average time to $O(h \cdot m)$. In practice, we can almost always find the optimal chain with $h = 50$; even if the heuristic fails, the optimal chain is often close.

For backtracking, let $P(i)$ be the index of the best predecessor of anchor i . It equals 0 if $f(i) = w_i$ or $\arg\max_j \{f(j) + \gamma(j, i) - \gamma(j, i)\}$ otherwise. For each anchor i in the descending order of $f(i)$, we apply $P(\cdot)$ repeatedly to find its predecessor and mark each visited i as ‘used’, until $P(i) = 0$ or we reach an already ‘used’ i . This way we find all chains with no anchors used in more than one chains.

In the absence of copy number changes, each query segment should not be mapped to two places in the reference. However, chains found at the previous step may have significant or complete overlaps due to repeats in the reference. Minimap2 used the following procedure to identify *primary chains* that do not greatly overlap on the query. Let Q be an empty set initially. For each chain from the best to the worst according to their chaining scores: if on the query, the chain overlaps with a chain in Q by 50% or higher percentage of the shorter chain, mark the chain as secondary to the chain in Q ; otherwise, add the chain to Q . In the end, Q contains all the primary chains. We did not choose a more sophisticated data structure (e.g. range tree or k-d tree) because this step is not the performance bottleneck.

2.2 Alignment

Minimap2 performs global alignment between adjacent anchors in a chain. It adopted difference-based formulation to derive alignment (Wu et al., 1996; Suzuki, 2016). When combined with SSE vectorization, this formulation has two advantages. First, because each score in the DP matrix is bounded by the gap cost and the maximum matching score, we can usually achieve 16-way SSE vectorization regardless of the peak score of the alignment. Second, filling the DP matrix along the diagonal, we can simplify banded alignment, which is critical to performance. In practice, our implementation is three times as fast as Parasail’s 4-way vectorization (Daily, 2016) for global alignment. Without banding, our implementation is slower than Edlib (Šošić and Škic, 2017), but with a 1000bp band, it is considerably faster. When performing global alignment between anchors, we expect the alignment to stay close to the diagonal of the DP matrix. Banding is often applicable.

Minimap2 uses a 2-piece affine gap cost $\gamma(l) = \min\{q + l \cdot e, \tilde{q} + l \cdot \tilde{e}\}$. On the condition that $q + e < \tilde{q} + \tilde{e}$ and $e > \tilde{e}$, this cost function is concave. It applies cost $q + l \cdot e$ to gaps shorter than $\lceil (\tilde{q} - q)/(e - \tilde{e}) \rceil$ and applies $\tilde{q} + l \cdot \tilde{e}$ to longer gaps. This scheme helps to recover longer insertions and deletions (INDEL; Gotoh, 1990).

With global alignment, minimap2 may force to align unrelated sequences between two adjacent anchors. To avoid such an artifact, we compute accumulative alignment score along the alignment path and break the alignment where the score drops too fast in the diagonal direction. More precisely, let $S(i, j)$ be the alignment score along the alignment path ending at cell (i, j) in the DP matrix. We break the alignment if there exist (i', j') and (i, j) , $i' < i$ and $j' < j$, such that

$$S(i', j') - S(i, j) > Z + e \cdot (\max\{i - i', j - j'\} - \min\{i - i', j - j'\})$$

where e is the gap extension cost and Z is an arbitrary threshold. This strategy is similar to X-drop employed in BLAST (Altschul et al., 1997).

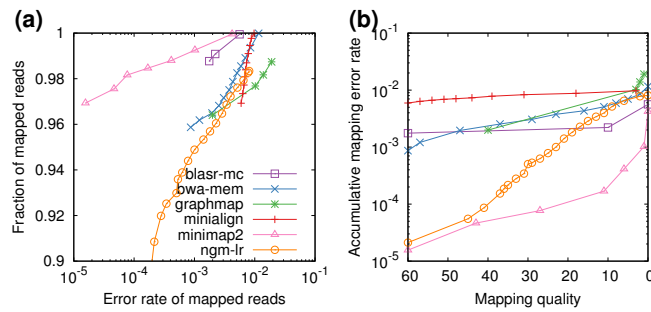


Fig. 1. Evaluation on simulated SMRT reads aligned against human genome GRCh38. (a) ROC-like curve. (b) Accumulative mapping error rate as a function of mapping quality. 33,088 \geq 1000bp reads were simulated using pbsim (Ono et al., 2013) with error profile sampled from file ‘m131017_060208_42213.*.1.*’ downloaded at <http://bit.ly/chm1p5c3>. The N50 read length is 11,628. A read is considered correctly mapped if the true position overlaps with the best mapping position by 10% of the read length. All aligners were run under the default setting for SMRT reads.

However, unlike X-drop, it would not break the alignment in the presence of a single long gap.

When minimap2 breaks a global alignment between two anchors, it performs local alignment between the two subsequences involved in the global alignment, but this time with the one subsequence reverse complemented. This additional alignment step may identify short inversions that are missed during chaining.

3 RESULTS

As a sanity check, we evaluated minimap2 on simulated human reads along with BLASR (Chaisson and Tesler, 2012), BWA-MEM (Li, 2013), GraphMap (Sović et al., 2016), minialign (Suzuki, 2016) and NGMLR (Sedlazeck et al., 2017). We excluded rHAT (Liu et al., 2016), LAMSA (Liu et al., 2017) and Kart (Lin and Hsu, 2017) because they either crashed or produced malformed output. In this evaluation, Minimap2 has higher power to distinguish unique and repetitive hits, and achieves overall higher mapping accuracy (Fig. 1a). It is still the most accurate even if we skip DP-based alignment (data not shown), suggesting chaining alone is sufficient to achieve high accuracy for approximate mapping. Minimap2 and NGMLR provide better mapping quality estimate: they rarely give repetitive hits high mapping quality (Fig. 1b). Apparently, other aligners may occasionally miss close suboptimal hits and be overconfident in wrong mappings. On run time, minialign is slightly faster than minimap2. They are over 30 times faster than the rest. Minimap2 consumed 6.1GB memory at the peak, more than BWA-MEM but less than others.

On real human SMRT reads, the relative performance and sensitivity of these aligners are broadly similar to those on simulated data. We are unable to provide a good estimate of mapping error rate due to the lack of the truth. On ONT ultra-long human reads (Jain et al., 2017), BWA-MEM failed. Minialign and minimap2 are over 70 times faster than others. We have also examined tens of \geq 100bp INDELs in IGV (Robinson et al., 2011) and can confirm the observation by Sedlazeck et al. (2017) that BWA-MEM often breaks them into shorter gaps. Minimap2 does not have this issue.

4 DISCUSSIONS

Minialign and minimap2 are fast because a) with chaining, they can quickly filter out most false seed hits (Li, 2016) and reduce unsuccessful but costly DP-based alignments; b) they implemented so far the fastest DP-based alignment algorithm for long sequences (Suzuki, 2016). It is possible to further accelerate minimap2 with a few other tweaks such as adaptive banding (Suzuki and Kasahara, 2017) or incremental banding.

In addition to reference-based read mapping, minimap2 inherits minimap’s ability to search against huge multi-species databases and to find read overlaps. On a few test data sets, minimap appears to yield slightly better miniasm assembly. Minimap2 can also align closely related genomes, though it would benefit from more thorough evaluations. Genome alignment is an intricate topic.

ACKNOWLEDGEMENTS

We owe a debt of gratitude to Hajime Suzuki for releasing his masterpiece and insightful notes before formal publication. We thank M. Schatz, P. Rescheneder and F. Sedlazeck for pointing out the limitation of BWA-MEM. We are also grateful to early minimap2 testers who have greatly helped to fix various issues.

REFERENCES

Abouelhoda, M. I. and Ohlebusch, E. (2005). Chaining algorithms for multiple genome comparison. *J. Discrete Algorithms*, 3:321–41.

Altschul, S. F. et al. (1997). Gapped BLAST and PSI-BLAST: a new generation of protein database search programs. *Nucleic Acids Res*, 25:3389–402.

Chaisson, M. J. and Tesler, G. (2012). Mapping single molecule sequencing reads using basic local alignment with successive refinement (BLASR): application and theory. *BMC Bioinformatics*, 13:238.

Daily, J. (2016). Parasail: SIMD C library for global, semi-global, and local pairwise sequence alignments. *BMC Bioinformatics*, 17:81.

Gotoh, O. (1990). Optimal sequence alignment allowing for long gaps. *Bull Math Biol*, 52:359–73.

Jain, M. et al. (2017). Nanopore sequencing and assembly of a human genome with ultra-long reads. *bioRxiv*. doi:10.1101/128835.

Langmead, B. and Salzberg, S. L. (2012). Fast gapped-read alignment with Bowtie 2. *Nat Methods*, 9:357–9.

Li, H. (2013). Aligning sequence reads, clone sequences and assembly contigs with BWA-MEM. *arXiv:1303.3997*.

Li, H. (2016). Minimap and miniasm: fast mapping and de novo assembly for noisy long sequences. *Bioinformatics*, 32:2103–10.

Lin, H.-N. and Hsu, W.-L. (2017). Kart: a divide-and-conquer algorithm for NGS read alignment. *Bioinformatics*.

Liu, B. et al. (2016). rHAT: fast alignment of noisy long reads with regional hashing. *Bioinformatics*, 32:1625–31.

Liu, B. et al. (2017). LAMSA: fast split read alignment with long approximate matches. *Bioinformatics*, 33:192–201.

Ono, Y. et al. (2013). PBSIM: PacBio reads simulator—toward accurate genome assembly. *Bioinformatics*, 29:119–21.

Robinson, J. T. et al. (2011). Integrative genomics viewer. *Nat Biotechnol*, 29:24–6.

Sedlazeck, F. J. et al. (2017). Accurate detection of complex structural variations using single molecule sequencing. *bioRxiv*. doi:10.1101/169557.

Šošić, M. and Škic, M. (2017). Edlib: a C/C++ library for fast, exact sequence alignment using edit distance. *Bioinformatics*, 33:1394–1395.

Sović, I. et al. (2016). Fast and sensitive mapping of nanopore sequencing reads with GraphMap. *Nat Commun*, 7:11307.

Suzuki, H. (2016). Fast and accurate alignment tool for pacbio and nanopore long reads. <https://github.com/ocxtal/minialign>.

Suzuki, H. and Kasahara, M. (2017). Acceleration of nucleotide semi-global alignment with adaptive banded dynamic programming. *bioRxiv*. doi:10.1101/130633.

Wu, S. et al. (1996). A subquadratic algorithm for approximate limited expression matching. *Algorithmica*, 15:50–67.

APPENDIX

A 2-piece gap cost function is

$$\gamma(l) = \min\{q + l \cdot e, \tilde{q} + l \cdot \tilde{e}\}$$

Without losing generality, we assume $q+e \leq \tilde{q}+\tilde{e}$. The equation to compute the optimal alignment under such a gap cost is (Gotoh, 1990)

$$\begin{cases} H_{ij} = \max\{H_{i-1,j-1} + s(i,j), E_{ij}, F_{ij}, \tilde{E}_{ij}, \tilde{F}_{ij}\} \\ E_{i+1,j} = \max\{H_{ij} - q, E_{ij}\} - e \\ F_{i,j+1} = \max\{H_{ij} - q, F_{ij}\} - e \\ \tilde{E}_{i+1,j} = \max\{H_{ij} - \tilde{q}, \tilde{E}_{ij}\} - \tilde{e} \\ \tilde{F}_{i,j+1} = \max\{H_{ij} - \tilde{q}, \tilde{F}_{ij}\} - \tilde{e} \end{cases} \quad (2)$$

where $s(i,j)$ is the score between the i -th reference base and j -th query base. If we define

$$\begin{cases} u_{ij} \triangleq H_{ij} - H_{i-1,j} & v_{ij} \triangleq H_{ij} - H_{i,j-1} \\ x_{ij} \triangleq E_{i+1,j} - H_{ij} & \tilde{x}_{ij} \triangleq \tilde{E}_{i+1,j} - \tilde{H}_{ij} \\ y_{ij} \triangleq F_{i,j+1} - H_{ij} & \tilde{y}_{ij} \triangleq \tilde{F}_{i,j+1} - \tilde{H}_{ij} \end{cases}$$

we can transform Eq. (2) to

$$\begin{cases} z_{ij} = \max\{s(i,j), x_{i-1,j} + v_{i-1,j}, y_{i,j-1} + u_{i,j-1}, \\ \tilde{x}_{i-1,j} + v_{i-1,j}, \tilde{y}_{i,j-1} + u_{i,j-1}\} \\ u_{ij} = z_{ij} - v_{i-1,j} \\ v_{ij} = z_{ij} - u_{i,j-1} \\ x_{ij} = \max\{0, x_{i-1,j} + v_{i-1,j} - z_{ij} + q\} - q - e \\ y_{ij} = \max\{0, y_{i,j-1} + u_{i,j-1} - z_{ij} + q\} - q - e \\ \tilde{x}_{ij} = \max\{0, \tilde{x}_{i-1,j} + v_{i-1,j} - z_{ij} + \tilde{q}\} - \tilde{q} - \tilde{e} \\ \tilde{y}_{ij} = \max\{0, \tilde{y}_{i,j-1} + u_{i,j-1} - z_{ij} + \tilde{q}\} - \tilde{q} - \tilde{e} \end{cases} \quad (3)$$

where z_{ij} is a temporary variable that does not need to be stored.

All values in Eq. (3) are bounded. To see that,

$$x_{ij} = E_{i+1,j} - H_{ij} = \max\{-q, E_{ij} - H_{ij}\} - e$$

With $E_{ij} \leq H_{ij}$, we have

$$-q - e \leq x_{ij} \leq \max\{-q, 0\} - e = -e$$

and similar inequations for y_{ij} , \tilde{x}_{ij} and \tilde{y}_{ij} . In addition,

$$u_{ij} = z_{ij} - v_{i-1,j} \geq \max\{x_{i-1,j}, \tilde{x}_{i-1,j}\} \geq -q - e$$

As the maximum value of $z_{ij} = H_{ij} - H_{i-1,j-1}$ is M , the maximal matching score, we can derive

$$u_{ij} \leq M - v_{i-1,j} \leq M + q + e$$

In conclusion, x and y are bounded by $[-q - e, -e]$, \tilde{x} and \tilde{y} by $[-\tilde{q} - \tilde{e}, -\tilde{e}]$, and u and v by $[-q - e, M + q + e]$. When matching score and gap cost are small, each of them can be stored as a 8-bit integer. This enables 16-way SSE vectorization regardless of the peak score of the alignment.

For a more efficient SSE implementation, we transform the row-column coordinate to diagonal-anti-diagonal coordinate by letting $r \leftarrow i + j$ and $t \leftarrow i$. Eq. (3) becomes:

$$\begin{cases} z_{rt} = \max\{s(t, r - t), x_{r-1,t-1} + v_{r-1,t-1}, y_{r-1,t} + u_{r-1,t}, \\ \tilde{x}_{r-1,t-1} + v_{r-1,t-1}, \tilde{y}_{r-1,t} + u_{r-1,t}\} \\ u_{rt} = z_{rt} - v_{r-1,t-1} \\ v_{rt} = z_{rt} - u_{r-1,t} \\ x_{rt} = \max\{0, x_{r-1,t-1} + v_{r-1,t-1} - z_{rt} + q\} - q - e \\ y_{rt} = \max\{0, y_{r-1,t} + u_{r-1,t} - z_{rt} + q\} - q - e \\ \tilde{x}_{rt} = \max\{0, \tilde{x}_{r-1,t-1} + v_{r-1,t-1} - z_{rt} + \tilde{q}\} - \tilde{q} - \tilde{e} \\ \tilde{y}_{rt} = \max\{0, \tilde{y}_{r-1,t} + u_{r-1,t} - z_{rt} + \tilde{q}\} - \tilde{q} - \tilde{e} \end{cases}$$

In this formulation, cells with the same diagonal index r are independent of each other. This allows us to fully vectorize the computation of all cells on the same anti-diagonal in one inner loop.

On the condition that $q + e < \tilde{q} + \tilde{e}$ and $e > \tilde{e}$, the boundary condition of this equation in the diagonal-anti-diagonal coordinate is

$$\begin{cases} x_{r-1,-1} = y_{r-1,r} = -q - e \\ \tilde{x}_{r-1,-1} = \tilde{y}_{r-1,r} = -\tilde{q} - \tilde{e} \\ u_{r-1,r} = v_{r-1,-1} = \eta(r) \end{cases}$$

where

$$\eta(r) = \begin{cases} -q - e & (r = 0) \\ -e & (r < \lceil \frac{\tilde{q}-q}{e-\tilde{e}} - 1 \rceil) \\ r \cdot (e - \tilde{e}) - (\tilde{q} - q) - \tilde{e} & (r = \lceil \frac{\tilde{q}-q}{e-\tilde{e}} - 1 \rceil) \\ -\tilde{e} & (r > \lceil \frac{\tilde{q}-q}{e-\tilde{e}} - 1 \rceil) \end{cases}$$

Suzuki (2016) first derived a similar set of equations under affine gap cost but with different notations.